

# Quasi-optimal PZT distribution in active vibration reduction of the triangular plate with P-F-F boundary conditions

ADAM BRAŃSKI and STANISŁAW SZELA

An active reduction of transverse vibration of the triangular plate with P-F-F boundary conditions is considered. The cracked plate is idealized research model as partially clamped on one edge with varying clamped length. The active reduction is realised with PZTs. In the paper, assuming the detached base clamped length, the influence of PZTs distribution on the bending moment and the shearing force at the clamped edge is investigated. To realize the purpose two cases are considered. At the former the PZTs are attached at points in which the curvatures of the surface locally take their maximum (MC sub-areas or quasi-optimal ones). At the latter, the PZTs are somewhat shifted. The plate is excited with harmonic plane acoustic wave. The second mode is considered only.

The active vibration reduction study with a finite element method (FEM) is carried out. The numerical calculations show that better results are obtained for MC distribution of the PZTs.

**Key words:** triangular plate, PZT (piezoelectric zirconate titanate actuator), P-F-F (partial-free-free) boundary condition, active vibration reduction

## 1. Introduction

An important contemporary technical problem is an active vibration reduction of mechanical structures. The vibration reduction of the beams, plates, shells [18, 23, 25] and rotating structures [19] plays a mayor part. The vibration reduction can be realized with piezoelectric zirconate titanate actuators (PZTs) [4, 5, 7, 9]. One of the most important problems is the distribution of PZTs on the structure. This problem is particularly difficult, if the structure has not either an axis or a point of symmetry. The best example of an unsymmetrical structure is the triangular plate.

The vibrations and its reduction of triangular plates are an important scientific problem in mechanics [6, 10, 21]. The effect of the cracked length on the dynamic behavior of the triangular plates was investigated in [16] and references cited therein. But only free

---

A. Brański is with Laboratory of Acoustic, Technical University of Rzeszow, Rzeszow, Poland, e-mail: [abranski@prz.rzeszow.pl](mailto:abranski@prz.rzeszow.pl). S. Szela is with Institute of Technology, University of Rzeszow, Rzeszow, Poland, e-mail: [szela@univ.rzeszow.pl](mailto:szela@univ.rzeszow.pl).

Received 30.09.2009.

vibrations of partial-free-free (P-F-F) cantilever plate were taken into account. The finite element method (FEM) was used in this study. The natural vibrations of the plates mentioned above were also determined experimentally in [20] and the results were compared with the FEM solution and published in [16].

The solution of the PZTs distribution problem on the triangular plate was solved in [1, 2]. It was proposed to bond of PZTs at surface places with maximum curvatures (MC); they were so called MC sub-areas or quasi-optimal ones (the solution is not optimal because the optimization theory was not applied). In [1, 2] the triangular plate with only clamped-free-free (C-F-F) boundary conditions was considered. So, the curvature of the plate surface might be determined in approximate manner, namely, the curvature of the cross section line of the plate perpendicular to the clamped edge was taken into account instead of the curvature of the surface. It was possible because this curvature is much greater than the ones in any other direction. But in the case of P-F-F boundary conditions, there is no direction of the dominated curvature. So, the curvature of the surface should be considered. It should be noted few papers on PZTs distribution on the vibration structure [8, 13, 14, 26]. But it is not pointed out the method of the problem solution. Furthermore, the symmetrical (in some sense) research objects are considered, viz. the beams and rectangular or square plates.

The aim of this paper is to confirm the idea of the MC distribution of PZTs to the active vibration reduction of the triangular plate with P-F-F boundary conditions. To realize the aim, the MC sub-areas must be determined based on curvature of the surface. An effect of the vibrations reduction is measured directly through the change of the vibration amplitude on the plate surface, bending moment and shearing force at the clamped edge. To do this, these quantities are calculated for two cases. In the first case PZTs are bonded at MC places. In the second case they are a bit shifted. The reduction effect is measured via appropriate coefficients. Note, that the reduction effect may be also measured indirectly, via parameter of the acoustic field radiated by the structure without and with PZTs acting [3, 12, 13, 14, 25, 26].

The validity of the idea of the MC distribution of PZTs is substantiated mathematically and numerically.

## 2. Formulation of plate theory

The governing equation of transverse vibration motion of the plate, on the basis of Kirchhoff's classical small deflection theory, has the following form [6, 15]

$$N\Delta^2 u + \rho h D_t^2 u = F \quad (1)$$

where:  $u = u(x, y, t)$  – transverse deflection,  $F = F(x, y, t)$  – external force,  $\rho$  – mass density,  $h$  – thickness,  $N = Yh^3/12(1 - \nu^2)$  – flexural rigidity,  $Y$  – Young's modulus,  $\Delta$  – Laplace's operator,  $\Delta = D_x^2 + D_y^2$ ,  $D_x^2(\cdot) = \partial^2(\cdot)/\partial x^2$ ,  $D_y^2(\cdot) = \partial^2(\cdot)/\partial y^2$ ,  $D_t^2(\cdot) = \partial^2(\cdot)/\partial t^2$ ,  $\nu$  – Poisson's ratio.

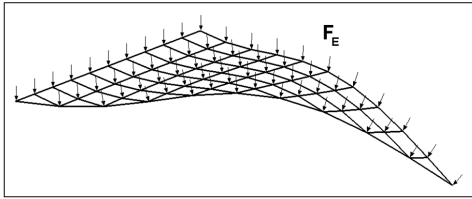


Figure 1. External loading by plane acoustic wave (numerical interpretation).

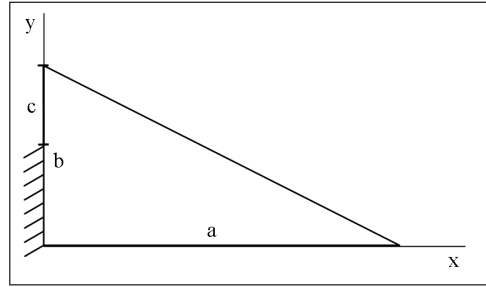


Figure 2. Triangular plate with P-F-F boundary conditions.

The external force consists of two components,

$$F = F_E + F_P \quad (2)$$

where:  $F_E = F_E(x, y, t)$  – external excitation forced by plane acoustic wave, Fig. 1,  $F_P = F_P(x, y, t)$  – control force due to PZTs.

The P-F-F boundary conditions imposed on the plate are defined in [11, 16, 20], Fig. 2. The boundaries at the clamped edge (b-edge) are described by

$$u = 0, \quad \theta = D_x u = 0. \quad (3)$$

For simplicity at free edges (a-, c- and d-edge respectively) the boundary conditions are described in compact form, i.e.

$$Q_x = 0, \quad M_{xx} = 0, \quad (4)$$

$$Q_y = 0, \quad M_{yy} = 0, \quad (5)$$

$$Q_n = 0, \quad M_{nn} = 0, \quad (6)$$

where  $Q_n$ ,  $Q_x$ ,  $Q_y$  – equivalent shear forces,  $M_{nn}$ ,  $M_{xx}$ ,  $M_{yy}$  – bending moments,  $\mathbf{n}$  – outside normal to the boundary,  $\mathbf{s}$  – outside tangential to the boundary,  $\alpha$  - the angle between normal  $\mathbf{s}$  and  $x$ -axis.

All calculations rely on FEM. This method is well-known (e.g. [17]). FEM is the base of ADINA computer code and this program was used.

### 3. Interaction between plate and PZTs

The system consists of the triangular plate and PZTs perfectly bonded to the plate surface. The mass and stiffness of PZTs are omitted, as they are far less than the same quantities of the plate. If PZT is excited, the interaction between PZT and the plate appears. The interaction process is presented in detail in [7, 9] and references cited therein.

The interaction leads to the reduction of the plate vibrations. Assuming the spatially uniform PZT, it provides boundary induction solely in terms of the external line moment distributed along the edges of the PZT [4, 22].

In the plate equation of motion (1), the action of PZT is given by [7, 9]

$$\begin{aligned}
 F_P = & -M_x (\langle x - x_1 \rangle^{-2} - \langle x - x_2 \rangle^{-2}) (\langle y - y_1 \rangle^0 - \langle y - y_2 \rangle^0) \\
 & -M_y (\langle y - y_1 \rangle^{-2} - \langle y - y_2 \rangle^{-2}) (\langle x - x_1 \rangle^0 - \langle x - x_2 \rangle^0)
 \end{aligned} \quad (7)$$

where  $\langle x \rangle^0 = H(x)$ ,  $\langle x \rangle^{-1} = \delta(x)$ ,  $\langle x \rangle^{-2} = \delta'(x)$ ,  $M_x$ ,  $M_y$  – line moments amplitudes [4].

The PZT induces bending moments in  $x$ - and  $y$ -direction. They are given by the formula

$$M_P = M_x = C_a \frac{d_{31}}{h_a} V, \quad M_y = C_a \frac{d_{32}}{h_a} V \quad (8)$$

where  $C_a$  – constant depending on geometry and mechanical properties of PZT and plate,  $d_{31}$ ,  $d_{32}$  – piezoelectric material strain constants,  $h_a$  – PZT thickness,  $V$  – voltage in the direction of polarization.

For example the bending moment along  $y$ -axis  $M_P = M_x$  is presented in Fig. 3(a). As the ADINA code is applied, the  $M_P$  must be replaced by the pair of linear forces, Fig. 3(b),

$$M_P = \frac{F_P l_P}{2} \quad (9)$$

where  $l_P = l_x$  – PZT length in  $x$ -direction. The acting of forces  $F_P$  on the plate models the acting of the PZT.

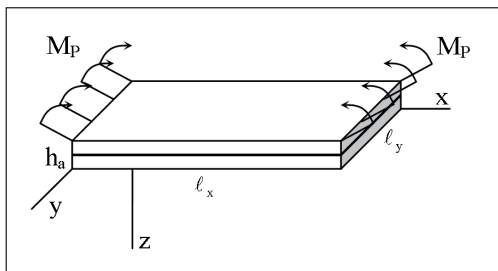


Figure 3. (a) Bending moments of PZT.

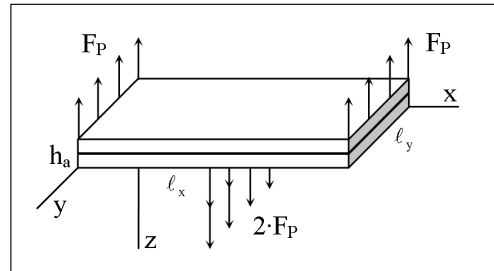


Figure 3. (b) Pair of forces of PZT.

#### 4. Curvature of the surface

The base of the surface curvature belongs to the theory of the differential geometry and its application to the plates may be found in [24]. For small deflections, the curvatures of the line, i.e. the cross section of the surface, in planes parallel to the planes  $\pi_{ux}$

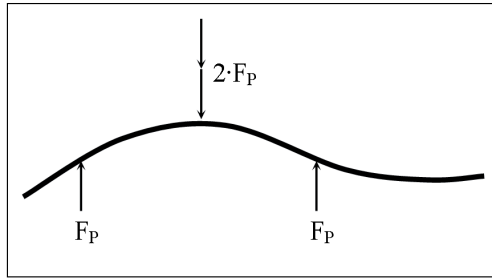


Figure 3. (c) Idea of the acting of PZTs on the plate.

and  $\pi_{uy}$  are given respectively by the formulas

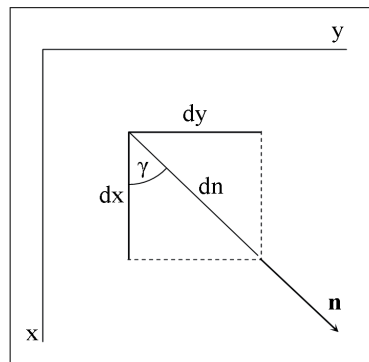
$$\kappa_x = -D_x^2 u \quad (10)$$

$$\kappa_y = -D_y^2 u. \quad (11)$$

In any direction, described by vector  $\mathbf{n}$ , the curvature is

$$\kappa_{\mathbf{n}} = \kappa_x \cos^2 \gamma - \kappa_{xy} \sin(2\gamma) + \kappa_y \sin^2 \gamma \quad (12)$$

where  $\gamma$  – see Fig. 4.

Figure 4. Definition of the angle  $\gamma$ .

The expression  $\kappa_{xy} = D_{xy}^2 u$  means twisting of the surface relatively to the  $x$ - and  $y$ -axis. The maximal curvature of the cross section line in any direction (main one) is the curvature of the surface at the point.

As mentioned above, in the case of C-F-F boundary conditions, the dominant curvature is given by Eq. (10), i.e. the curvature of the line perpendicular to the clamped edge. In the case of P-F-F boundary conditions, the curvature in all directions is similar. Hence, the surface curvature should be analyzed from Eq. (12) instead of line one. In the

following analysis, the surface extreme curvatures, in the direction  $\gamma$  play a major part, i.e.  $\kappa_{ext}(\kappa_{max}, \kappa_{min})$ ,

$$\left. \begin{array}{l} \kappa_{max} \\ \kappa_{min} \end{array} \right\} = \frac{1}{2} \left( \kappa_x + \kappa_y \pm \left( (\kappa_x - \kappa_y)^2 + \kappa_{xy}^2 \right)^{1/2} \right). \quad (13)$$

The curvatures  $\kappa_{max}$  and  $\kappa_{min}$  are placed in the planes which are perpendicular each other. In numerical calculations, one has to disposal the sets of discrete values  $\{x_i, y_i\}$  and  $\{u(x_i, y_i)\}$  rather than the function  $u = u(x, y)$ ;  $x_i, y_i$  – nodes,  $i = 1, 2, \dots$ . So, instead of (13) its discrete form is used as follows:

$$\left. \begin{array}{l} \kappa_i \max \\ \kappa_i \min \end{array} \right\} = \frac{1}{2} \left( \kappa_{x_i} + \kappa_{y_i} \pm \left( (\kappa_{x_i} - \kappa_{y_i})^2 + \kappa_{x_i y_i}^2 \right)^{1/2} \right). \quad (14)$$

The derivatives are replaced by appropriate finite differences (hereafter central ones)

$$\kappa_{x_i} = -\frac{u_{x_{i-1}, y_j} - 2u_{x_i, y_j} + u_{x_{i+1}, y_j}}{h_x^2} \quad (15)$$

$$\kappa_{y_i} = -\frac{u_{x_i, y_{i-1}} - 2u_{x_i, y_i} + u_{x_i, y_{i+1}}}{h_y^2} \quad (16)$$

$$\kappa_{x_i y_i} = \frac{u_{x_{i+1} y_{j+1}} - u_{x_{i-1} y_{j+1}} - u_{x_{i+1} y_{j-1}} + u_{x_{i-1} y_{j-1}}}{4 h_x h_y} \quad (17)$$

where  $h_x, h_y$  – distance between nodes in  $x$ -direction and in  $y$ -direction respectively.

## 5. Quasi-optimal places

As depicted in Fig. 3(b), two sets of line forces are in the disposal, i.e.  $\{F_x, F_y\}$ ,  $\{2F_x, 2F_y\}$ . The idea of MC distribution of the PZT is as follow. Put the forces  $\{2F_x, 2F_y\}$  on the line parallel to the  $x$ -,  $y$ -axis respectively. The intersection of these lines lies at the point of the plate surface with maximum curvature Fig. 3(c). This point is so-called MC one and consequently the PZT is MC distributed. Strictly speaking, PZT covers some surface of the plate. This sub-area is called MC one. The forces  $\{F_x, F_y\}$  of each pair have to be distributed symmetrically to the appropriate line. In these circumstances, the plate is maximum "unbended".

The above explanation of MC distribution concerns only one PZT. However, it is valid in more general case. If the surface has two or more points with maximum locally curvatures, more PZTs should be bonded at these points in the similar manner.

## 6. The reduction and effectiveness coefficients

Let be the difference between some physical values at the point of the suitable area

$$\Delta\Psi = \Psi - \Psi_P \quad (18)$$

where  $\Psi$  and  $\Psi_P$  – values of quantities calculated without and with PZT respectively,  $\Psi = \{A, M, Q\} - \{\text{vibration amplitude, bending moment, shearing force}\}$ . The difference  $\Delta\Psi$  is interpreted as the quantity of the vibration reduction and it is the first measure of this reduction, i.e. the quantity reduction coefficient.

The second measurement of the vibration reduction is defined as

$$R_\Psi = \frac{\Delta\Psi}{\Psi} = \frac{\Psi - \Psi_P}{\Psi}. \quad (19)$$

$R_\Psi$  is called the reduction coefficient and may be expressed in percent. Note, that if the reduction coefficient is equal to one, the vibrations are entirely reduced.

An effectiveness of the vibration reduction is defined as a quotient of some vibration reduction measure by an amount of an energy provided to the system in order to excite PZT. Hence, thurst measurement of the vibration reduction may be defined by the following formula

$$R_{E;\Psi} = \frac{R_\Psi}{W} \quad (20)$$

where  $W$  – amount of the energy provided to the system in order to excite PZT.

The  $R_{E;\Psi}$  is called an effectiveness coefficient. Energy provided to the system is translated into couples of forces, Fig. 3(b). Therefore, the energy  $W$  in (20) may be replaced with forces  $F_P$ , hence

$$R_{E;\Psi} = \frac{R_\Psi}{f_\Sigma} \quad (21)$$

where  $f_\Sigma = \sum_P F_P$ ,  $P = 1, 2, \dots, n_P$ ,  $n_P$  – number of actuators PZT in the system.

Hereafter for each PZT only one value of  $F_P$  in denominator of (21) is taken into account. The results will be similar, if this rule is retained for each case.

Eqs. (18)-(21) define the appropriate factors of the vibration reduction at the point of the given area. In many cases, it is convenient to calculate mean values of these factors at all area or at sub-areas. First of them is the mean value of quantity of the vibration reduction or briefly the mean quantity reduction coefficient. It is defined by the following formula

$$\Delta\Psi_m = \frac{1}{n_i} \sum_i (\Psi_i - \Psi_{P;i}), \quad i = 1, 2, \dots, n_i \quad (22)$$

where  $\Psi_i$  and  $\Psi_{P;i}$  – values of quantities calculated without and with PZT respectively at  $i$ -points of the area,  $n_i$  – number of points. Consequently, the mean reduction coefficient and the mean effectiveness coefficient are defined respectively

$$R_{\Psi_m} = \frac{\Delta\Psi_m}{\Psi_m} \quad (23)$$

$$R_{E;\psi_m} = \frac{R_{\psi_m}}{W} \quad (24)$$

or

$$R_{E;\psi_m} = \frac{R_{\psi_m}}{f_{\Sigma}} \quad (25)$$

where  $\psi_m = 1/n_i \sum_i \psi_i$ . Hereafter, it is used only these factors which are appropriate to the considered problem.

## 7. Numerical calculations and results

As mentioned in the introduction, for the MC distribution of PZT and C-F-F boundary conditions the numerical results and conclusions are presented in [1, 2] and will not be repeated here. Hereafter, to emphasize the validation and effectiveness of MC distribution of PZTs on the triangular plate with P-F-F boundary conditions, the sets of numerical experiments are performed. So, MC sub-areas is searched via the local maximal curvature of the plate surface, but not through the appropriate line curvature as in [1, 2].

As a research object the plate made from aluminium with thickness  $h = 0.0625$  in (1.59 [mm]) is taken into account [1, 2, 20]. The length  $b$ , without the crack  $c$  is taken as  $b = 10$  [in] (254 [mm]) and the free edge  $a = 15$  [in] (381 [mm]). The material constants used for calculations are assumed as follows: density  $\rho = 0.259$  [lb/in<sup>3</sup>] (7169 [kg/m<sup>3</sup>]), Young's modulus  $Y = 10.4 \times 10^6$  [psi] (71.7 [GPa]), Poisson's ratio  $\nu = 0.32$ . For the PZTs: the piezoelectric strain constant  $d_{31} = d_{32} = -190 \times 10^{-12}$  [m/V] and thickness  $h_a = 0.019$  [in] (0.48 [mm]), density  $\rho_a = 0.282$  [lb/in<sup>3</sup>] (7800 [kg/m<sup>3</sup>]), Young's modulus  $Y = 9.57 \times 10^6$  [psi] (66 [GPa]) and Poisson's ratio  $\nu_a = 0.34$ .

The vibrations are forced with the loudspeaker in form of plane acoustic wave, harmonic in time and second frequency. Such external loading is uniformly distributed on the plate, Fig. 1. The second frequency is only chosen, because the first mode (for the first frequency) has one global point with maximum curvature, hence this case is less interesting. In turn, the third and next modes, are more complicated and the proof of the idea of MC distribution of PZTs should have been somewhat technical difficult. Furthermore, the higher frequencies play a minor part in the vibration. The numerical simulations are carried out for the set of the crack length viz.  $c = \{0.4, 0.6, 0.8\} \cdot b$ . It is obvious, that for three examined examples (three length of the clamped edge) the second frequency is the set  $f = \{67.8, 50.0, 29.9\}$  [Hz].

The surface curvature is determined on the base of (14). For this purpose, the net of points is covered of the plate surface: 481 points in the  $x$ -direction and 321 points in  $y$ -direction. At each point of the net, 64 directions described by angle  $\gamma$  are chosen,  $\gamma = [0, \dots, 180^0]$ , Fig. 4. Next, at each point and at each direction the curvature of the cross section lines is calculated. The maximal curvature of the line out of the set line curvatures makes up the curvature of the surface at the net point. Surrounding of this point is called MC sub-area.

For the second mode there is one MC sub-area with dominating curvature. At this sub-area, one square PZT is placed. Its dimensions are  $\ell_x \times \ell_y = 0.0254 \times 0.0254$  [m]. To compare the results, the calculations for shifted PZT about  $\ell_x$  long are performed. It is worth to stress, that the numerical calculations are performed for number of different distributions of PZT obtained by shifting it in different directions and the different distance in relation to the MC distribution. In the paper the results for one shift of PZT are presented since the other ones are the same in terms of the quality.

The interaction between PZT and plate is modeled with the forces put to PZT edges. Values of these forces, the same at the opposite edges, are different on the perpendicular edges. Their values focused on the PZT edges parallel to the  $x$ - and  $y$ -axis are different for separate cracks and they are as follows:  $[f_x, f_y] = [2, 0.5]$  [N],  $[1, 1]$  [N] and  $[1, 2.5]$  [N].

Hereafter, the comments to the calculated results are given only to the first block (i.e. for the crack  $c = 0.4b$ ) pointing out appropriate rest results (for  $c = \{0.5, 0.8\}b$ ). The second mode of the plate with the crack  $c = 0.4b$  is depicted in Fig. 5(a) (Figs. 6(a) and 7(a)). The curvatures of the plate surface are shown in Fig. 5(b) (Figs. 6(b) and 7(b)). There are two clear sub-areas with locally maximal curvatures of the plate surface. But at the sub-area, in the vicinity of the crack, the curvature achieves definitely dominant value. At this place, exactly in which the curvature achieves the global maximum, one PZT is bonded. It is marked by the black square and MC label in Fig. 5(c) (Figs. 6(c) and 7(c)). In this sub-area the maximal curvature is exactly on the clamped line. Therefore, from a technical point of view, PZT is shifted about necessary distance  $\ell_x/2$ . To compare the vibration reduction, the PZT is shifted about distance  $\ell_x$  relatively to MC distribution. It is shown in Fig. 5(c) (Figs. 6(c) and 7(c)) with grey square and SF label.

Because of the special object of research, the vibration reduction is measured in two ways. First, it is measured through an analysis of the vibration amplitude  $A(x, y)$  of the plate surface. Second, it is measured through an analysis of the bending moment  $M_{xx}(x = 0, y)$  and the shearing force  $Q_x(x = 0, y)$  at the clamped edge. From technical point of view, the aim of the vibration reduction is mainly the reduction of  $M_{xx}(x = 0, y)$  and  $Q_x(x = 0, y)$ . But the amplitude reduction is also analyzed because its reduction is translated into the reduction of two rest quantities.

The reduction magnitude of the vibration amplitude  $\Delta A$  for MC distribution is presented in Fig. 5(d) (Figs. 6(d) and 7(d)). However,  $\Delta A$  for SF distribution is depicted in Fig. 5(e) (Figs. 6(e) and 7(e)). First set of results (concern to  $\Delta A$ ) is pointed out: the reduction for MC distribution of PZT is much bigger (hot colors) than the reduction for SF distribution. For both distributions of PZT, but particular for MC one, the sub-area of reduction amplitude is moved, together with the increase of the crack length, towards the free plate vertex of the crack edge. Note, that there are also little strengthening sub-areas of the vibration amplitude (inside black line), mainly in neighborhood of the clamped edge. But for the plate with P-F-F boundary conditions the strengthening sub-areas are considerably smaller than for the plate with C-F-F [1, 2]. These remarks are confirmed also by the reduction coefficient  $R_A$ . It is shown in Fig. 5(f) (Figs. 6(f) and 7(f)).

The bending moment  $M_{xx}$  and shearing force  $Q_x$  at the clamped edge are depicted in Figs. 5(h), 5(i) (Figs. 6(h), 6(i) and 7(h), 7(i)). For both distributions of PZT, the

reduction of  $M_{xx}$  and  $Q_x$  is observed almost along all length of clamped edge. It should be emphasized that the reduction of both quantities is much greater for MC distribution in comparison with SF distribution.

The mean reduction coefficients are gathered in Tab. 1. If the geometric-physical parameters of the PZT are the same for MC and SF distributions then the reduction and effectiveness coefficients are also the same and the latter are omitted. One can conclude from tab. 1 that the obtained results confirm greater vibration reduction, and consequently greater vibration effectiveness for the MC distribution of the PZT in comparison with SF distribution.

### 7.1. Vibration reduction for $c = 0.4b$

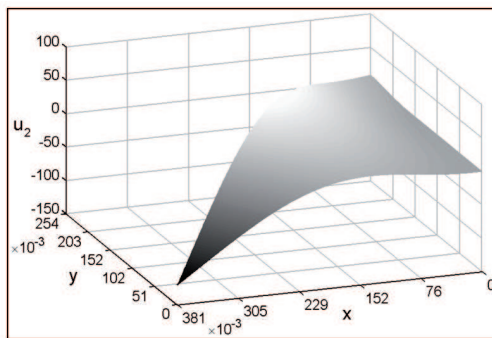


Figure 5. (a) Second mode,  $c = 0.4b$ .

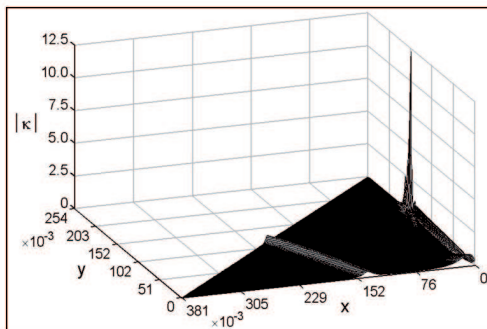


Figure 5. (b) Surface curvatures.

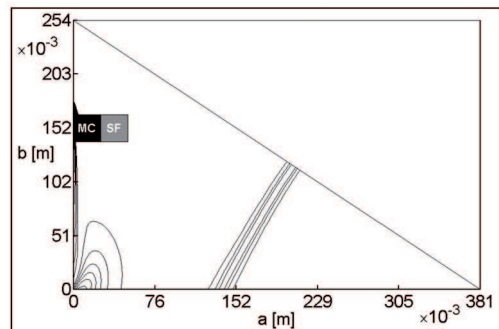


Figure 5. (c) Distribution of PZTs.

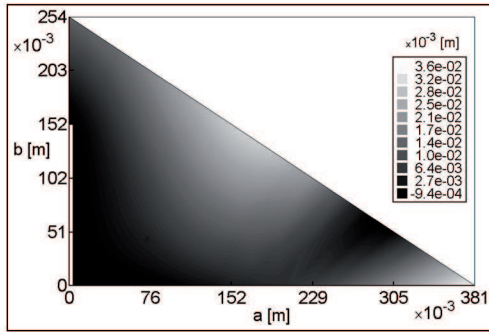
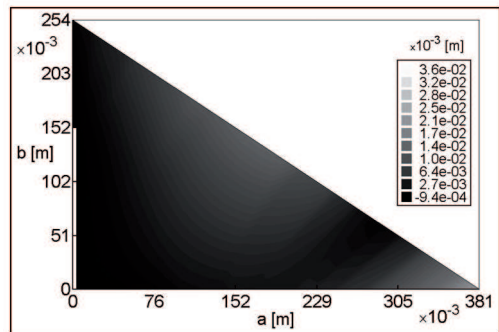
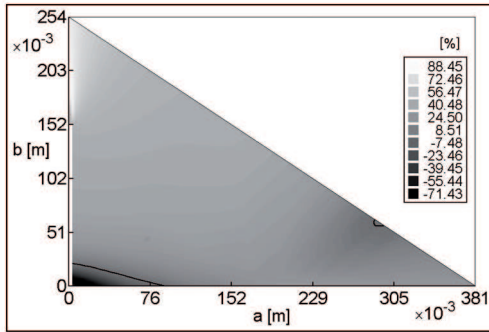
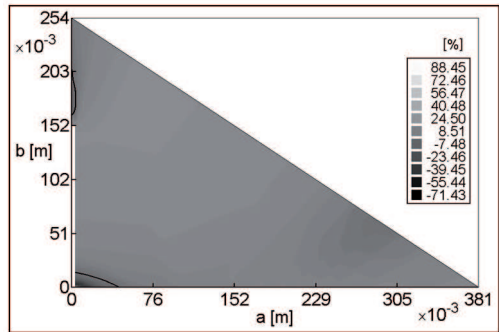
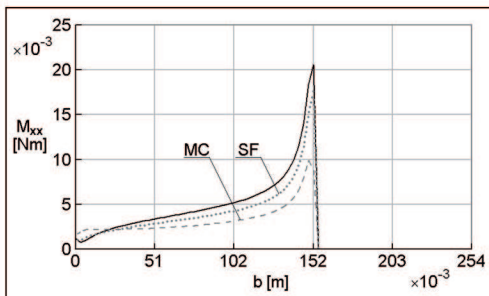
Figure 5. (d) Reduction magnitude  $\Delta A$  for MC.Figure 5. (e) Reduction magnitude  $\Delta A$  for SF.Figure 5. (f) Reduction coefficient  $R_A$  for MC.Figure 5. (g) Reduction coefficient  $R_A$  for SF.

Figure 5. (h) Bending moment at the clamped edge, line: solid – without reduction, dashed – MC, dotted – SF.

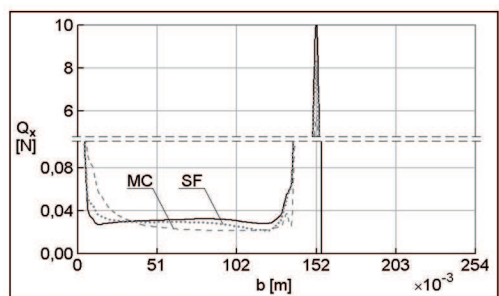


Figure 5. (i) Shearing force at the clamped edge, line: solid – without reduction, dashed – MC, dotted – SF.

**7.2. Vibration reduction for  $c = 0.6b$**

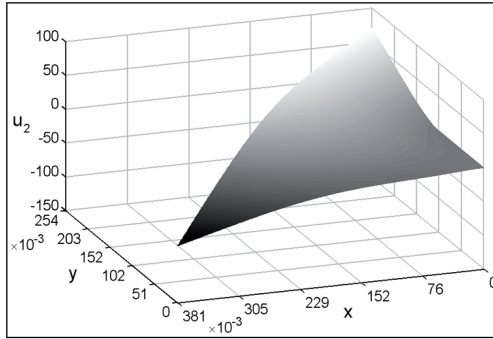


Figure 6. (a) Second mode,  $c = 0.6b$ .

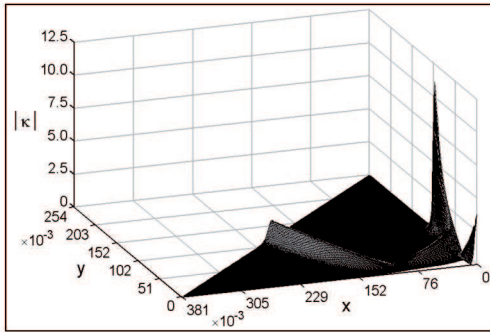


Figure 6. (b) Surface curvatures.

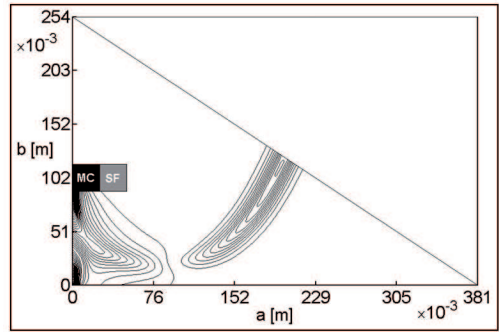


Figure 6. (c) Distribution of PZTs.

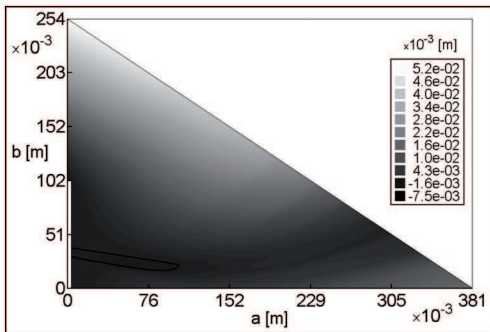


Figure 6. (d) Reduction magnitude  $\Delta A$  for MC.

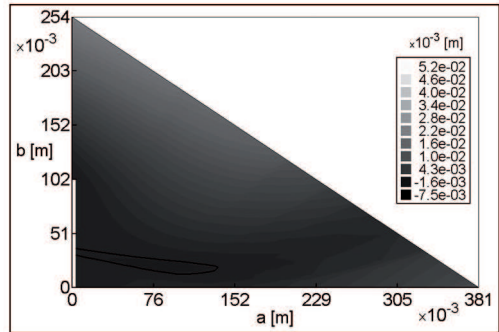


Figure 6. (e) Reduction magnitude  $\Delta A$  for SF.

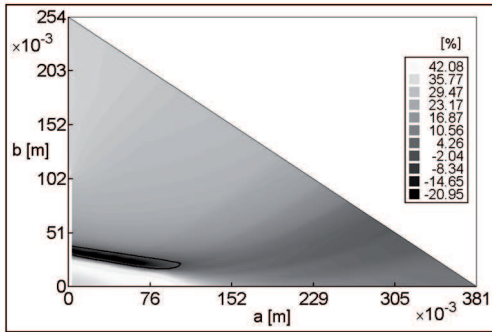


Figure 6. (f) Reduction coefficient  $R_A$  for MC.

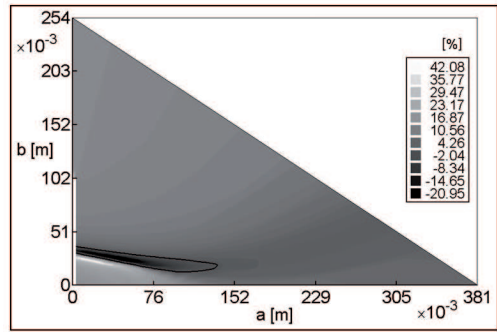


Figure 6. (g) Reduction coefficient  $R_A$  for SF.

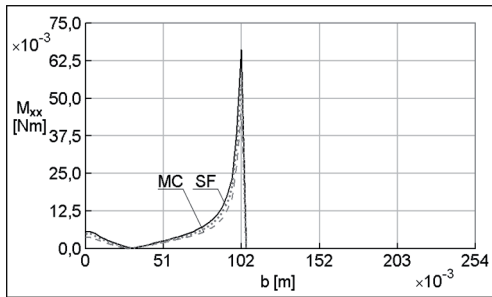


Figure 6. (h) Bending moment at the clamped edge, line: solid – without reduction, dashed – MC, dotted – SF.

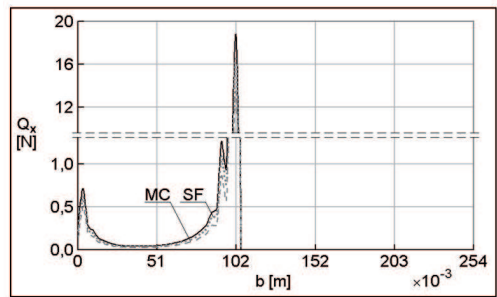


Figure 6. (i) Shearing force at the clamped edge, line: solid – without reduction, dashed – MC, dotted – SF.

### 7.3. Vibration reduction for $c = 0.8b$

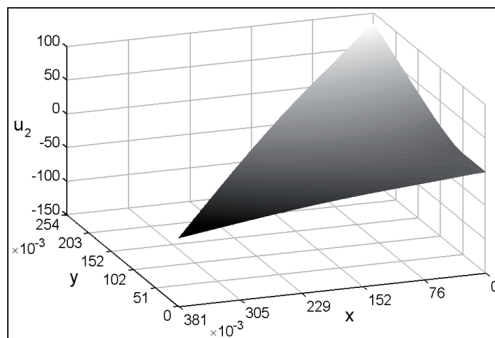


Figure 7. (a) Second mode,  $c = 0.8b$ .

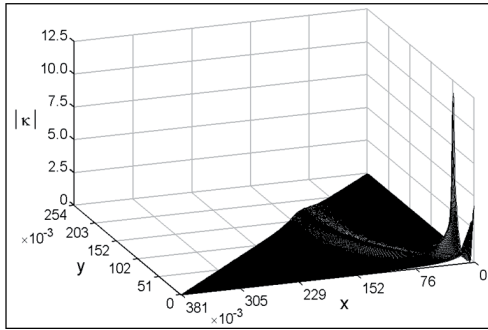


Figure 7. (b) Surface curvatures.

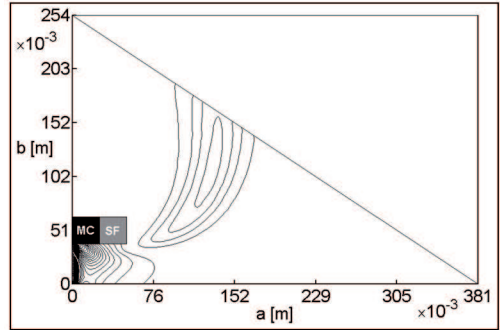


Figure 7. (c) Distribution of PZTs.

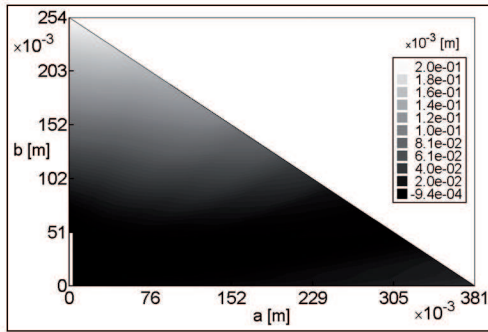


Figure 7. (d) Reduction magnitude  $\Delta A$  for MC.

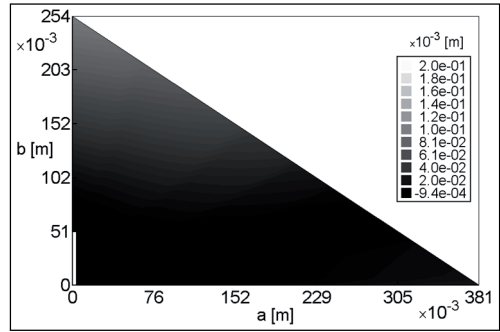


Figure 7. (e) Reduction magnitude  $\Delta A$  for SF.

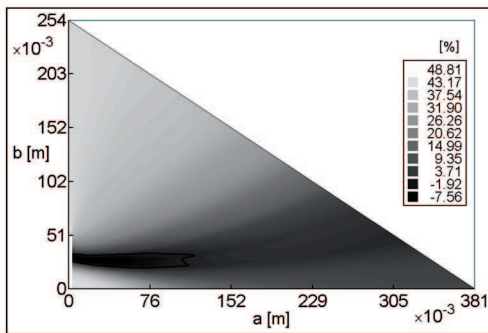


Figure 7. (f) Reduction coefficient  $R_A$  for MC.

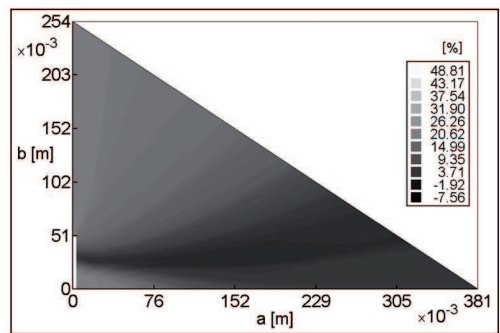


Figure 7. (g) Reduction coefficient  $R_A$  for SF.

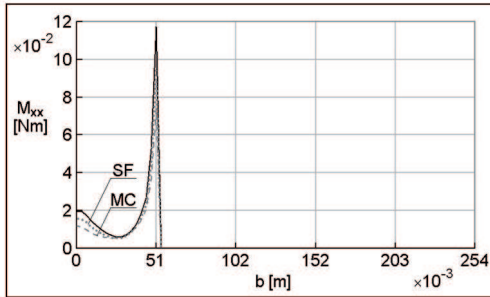


Figure 7. (h) Bending moment at the clamped edge, line: solid – without reduction, dashed – MC, dotted – SF.

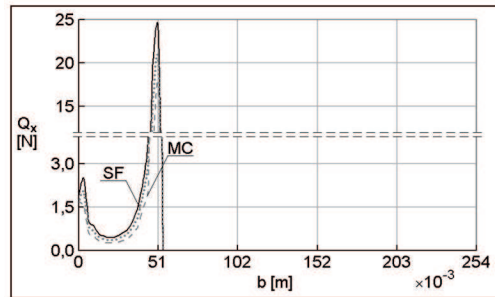


Figure 7. (i) Shearing force at the clamped edge, line: solid – without reduction, dashed – MC, dotted – SF.

#### 7.4. Mean coefficients of the vibration reduction

Table 3. Mean coefficients of the vibration reduction

c	Coefficients	MC	SF
0.4b	$R_{A_m}$	31.3 %	14.2 %
	$R_{M_{xx;m}}$	36.1 %	16.1 %
	$R_{Q_{x;m}}$	28.2 %	11.1 %
0.6b	$R_{A_m}$	21.3 %	9.4 %
	$R_{M_{xx;m}}$	27.8 %	12.7 %
	$R_{Q_{x;m}}$	38.0 %	16.5 %
0.8b	$R_{A_m}$	23.9 %	12.3 %
	$R_{M_{xx;m}}$	31.0 %	17.1 %
	$R_{Q_{x;m}}$	43.1 %	20.9 %

## 8. Conclusions

Theory and numerical calculations lead to the following conclusions:

1. The PZTs, in active vibration reduction of triangular plates, should be bonded in the special sub-areas, so called quasi-optimal ones. The quasi-optimal places pointed out the local or global maximum curvatures of the surface.

2. The quasi-optimal distribution of PZTs gives better effect than the other one. The effect is measured, via appropriate coefficients, by the reduction of the vibration amplitude on whole plate surface, the bending moment and the shearing force at the clamped edge. This and the first conclusion confirm the results published in [1] and [2].
3. In the vicinity of the crack, the curvature achieves maximal value. At this place, i.e. quasi-optimal sub-area, one PZT should be attached.
4. If the crack is increased, the sub-area of maximal reduction amplitude is moved towards the free plate vertex of the crack edge. This conclusion is obvious because for the plate with C-F-F boundary conditions, the maximal vibration amplitude is at the free plate vertex. For the plate with crack the maximal vibration amplitude is at free plate vertex but of the crack edge. Therefore in active vibration reduction in these (different) places, the greatest amplitude vibration reduction appears.
5. The strengthening sub-areas of the vibration amplitude are mainly in neighborhood of the clamped edge and they are smaller than for the plate with C-F-F boundary conditions.
6. The significant increase of the bending moment and shearing force in the clamped edge is noted at the vicinity of the point junction clamping-crack. The phenomenon is caused by the notch and it is increased together with the increase of the crack length. Application of the active vibration reduction causes significant decreasing of these quantities.
7. Mean reduction coefficients for the plate with P-F-F boundary conditions are greater than with C-F-F ones. It means that the vibration reduction and the effectiveness reduction at the first case are greater too.

The conclusions entirely confirm the value of the idea of quasi-optimal distribution of PZTs on triangular plates with P-F-F boundary conditions in the vibration reduction problem.

### References

- [1] A. BRAŃSKI and S. SZELA: On the quasi optimal distribution of PZTs in active reduction of the triangular plate vibration. *Archives of Control Sciences*, **17**(4), (2007), 427-437.
- [2] A. BRAŃSKI and S. SZELA: Improvement of effectiveness in active triangular plate vibration reduction. *Archives of Acoustics*, **33**(4), (2008), 521-530.

- [3] A. BRAŃSKI and S. SZELA: Evaluation of active vibration reduction of the triangular plate via acoustic field parameter. *Open Seminar on Acoustics*, Rzeszow-Przemyśl, Poland, (2007), 162-163, ISBN 83-91439-10-1.
- [4] S.E. BURKE and J.E. HUBBARD: Distributed transducer vibration control of thin plates. *J. of the Acoustical Society of America*, **90**(2,) (1991), 937-944.
- [5] M.J. CROKER: Handbook of noise and vibration control. Australia, John Wiley & Sons, 2007. ISBN 97-80471-39599-7.
- [6] S. CHAKRAVERTY: Vibration of plates. Boca Raton, London, New York, CRC Press, 2009, ISBN 97-81420-05395-1.
- [7] C.R. FULLER, S.J. ELLIOT and P.A. NIELSEN: Active control of vibration. London, Academic Press, 1997, ISBN 97-80122-69440-0.
- [8] Z. GOSIEWSKI and A. KOSZEWNİK: The influence of the piezoelements placement on the active vibration damping system. *Active Noise and Vibration Control Methods*, Krakow-Krasiczyn, Poland, (2007), 69-79, ISBN 83-89772-41-8.
- [9] C.H. HANSEN and S.D. SNYDER: Active control of noise and vibration. London, E&FN SPON, 1997, ISBN 04-19193-90-1.
- [10] W. KARUNASENA, S. KITIPORNCHAI and F.G.A. AL.-BERMANI: Free vibration of cantilevered arbitrary triangular Mindlin plates. *Int. J. of Mechanical Sciences*, **38**(4), (1996), 431-442.
- [11] S.W KANG and J.M. LEE: Free vibration analysis of arbitrarily shaped plates with clamped edges using wave-type functions. *J. of Sound and Vibration*, **242**(1), (2001), 9-26, ISSN 0022-460X.
- [12] M.S. KOZIEŃ: Acoustic radiation of plates and shallow shells. Krakow, Cracow University of Technology, 2006, ISSN 0860-097X.
- [13] M.S. KOZIEŃ and J. WICIAK J: Acoustics radiation of a plate with line and cross type piezoelectric elements. *Molecular and Quantum Acoustics*, **24** (2003), 97-108, ISSN 1731-8505.
- [14] M.S. KOZIEŃ and J. WICIAK: Impact analysis of piezoelectric elements distribution on the acoustic radiation of the plate. *Open Seminar on Acoustics*, Gliwice-Szczyrk, Poland, (2003), 245-248, ISSN 0137-5075, (in Polish).
- [15] A.W. LEISSA: Vibration of plates. Washington, NASA SP-160, D.C.: Office of Technology Utilization, 1969, Document ID 19700009156.
- [16] S. MIRZA and Y. ALIZADEH: Free vibration of partially supported triangular plates. *Computers & Structures*, **51**(2), (1994), 143-150, ISSN 0045-7949.

- 
- [17] S. MOAVENI: Finite element analysis. Theory and application with ANSYS. Pearson, Prentice Hall, 2008, ISBN 97-80131-89080-0.
- [18] M. PIETRZAKOWSKI: Active damping of transverse vibration using distributed piezoelectric elements. Oficyna Wydawnicza Politechniki Warszawskiej, Warsaw, Poland, 2004, ISSN 0137-2335.
- [19] P.M. PRZYBYŁOWICZ: Piezoelectric vibration control of rotating structures. Oficyna Wydawnicza Politechniki Warszawskiej, Warsaw, Poland, 2002, ISSN 0137-2335.
- [20] R. SINGHAL and D. REDEKOP: Vibration of right-angled triangular plates partially clamped on one side. *J. of Sound and Vibration*, **251**(2), (2002), 377-382, ISSN 0022-460X.
- [21] T. SAKIYAMA and M. HUANG: Free-vibration analysis of right triangular plates with variable thickness. *J. of Sound and Vibration*, **234**(5), (2000), 841-858, ISSN 0022-460X.
- [22] J.M. SULLIVAN, J.E. HUBBARD and S.E. BURKE: Modeling approach for two-dimensional distributed transducers of arbitrary spatial distribution. *J. of the Acoustical Society of America*, **99**(5), (1996), 2965-2974, ISSN 0001-4966.
- [23] A. TYLIKOWSKI: Control of circular plate vibrations via piezoelectric actuators shunted with a capacitive circuit. *Thin-Walled Structures*, **39** (2001), 83-94, Doi 10.1016/S0263-8231(00)00055-0.